In silico Local Impedance Mapping Using Multielectrode Catheters

Carmen Martínez Antón[1], Laura Anna Unger[2], Axel Loewe[1], Olaf Dössel[1]

[1] Institute of Biomedical Engineering, Karlsruhe Institute of Technology (KIT), Karlsruhe, Germany
[2] Medizinische Klinik IV, Städtisches Klinikum Karlsruhe, Karlsruhe, Germany

Abstract

Mapping techniques are currently used to estimate the location of atrial substrate potentially causing atrial fibrillation. Local impedance (LI) has recently gained attention as another modality for atrial substrate assessment as it does not rely on the dynamically changing electric activity of the heart. However, its potential has been mainly studied using point-by-point acquisitions disregarding multielectrode mapping catheters. This study explores the ability of LI to assess catheter-tissue contact and identify healthy and scar tissue using in silico models of two multielectrode mapping catheters. Combining three tissue configurations, five catheter-tissue distances, and 13 different stimulating bipoles, simulated LI values were computed. Increasing the catheter-tissue distance yielded monotonously decreasing LI values, whereas the presence of a scar line altered the LI measurements compared to the homogeneous patches. We conclude that in silico multielectrode LI measurements can help identifying direct catheter-tissue contact and distinguishing between healthy or scar tissue underneath, paving the way towards their use as a surrogate for atrial substrate assessment in clinical mapping applications.

1. Introduction

Atrial fibrillation (AF) is a heart condition whose treatment remains a challenge, especially in patients showing severely remodeled substrate. Regions of scar and fibrotic tissue have been identified as potential causes of arrhythmic activity, rendering them potential ablation targets. High density mapping techniques can provide important information about low voltage and slow conduction zones, common characteristics of these areas, but these modalities still show discordances in the location and extent of arrhythmogenic areas [1].

Recently, LI measurements have gained attention in radiofrequency ablation and substrate characterization as they are expected to distinguish between healthy and scar tissue independently from the atrial rhythm, which can improve the understanding of underlying substrate. The DirectSense™ technology [2] (Boston Scientific) integrated into the Rhythmia HDx electroanatomical mapping system (Boston Scientific), provides bipolar impedance measurements on an ablation catheter without involving a reference skin electrode. This technology determines only point-by-point values obtained at the tip of the catheter, but can serve as a starting point to extend the concept towards mapping. The main advantage lies in having two distinct pairs of electrodes as part of the injection and measurement circuit, which minimizes the impact of contact impedance between the electrode and the tissue.

Beyond characterizing cardiac tissue for distinguishing between healthy myocardium and fibrotic or scar tissue [3], LI has also been studied as a surrogate to assess catheter-tissue contact without needing a force module. In previous studies, an *in silico* framework with ablation catheters has been developed and used to evaluate LI confounding factors [4, 5]. Unger et al. [6] also demonstrated the potential use of LI by acquiring full-chamber atrial point-by-point LI maps. Thus, the integration of LI measurements into multielectrode catheters may show benefit for tissue characterization when combined with widely used methods such as voltage mapping.

This work explores *in silico* LI measurements using the layout of a multielectrode mapping catheter. Located on a simple myocardial tissue patch, different electrodes of the catheter serve as parts of the stimulating and measuring bipolar pairs to acquire a full map characterizing the substrate.

2. Methods

2.1. Geometrical Setup

As illustrated in Figure 1, a tissue patch measuring 70 mm × 70 mm × 2.5 mm was embedded into a box of blood of dimensions 100 mm × 100 mm × 100 mm.

Two different high density mapping catheters, namely the Advisor™ HD Grid (Abbott) and the PentaRay™ (Biosense Webster), were placed centrally above the tissue patch. The electrodes of either catheter were represented as spheres with radius $r_S = 0.5$ mm. De-

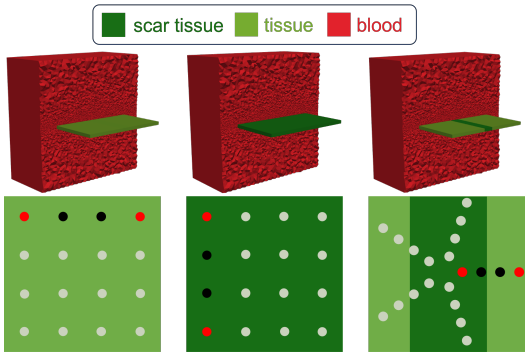

Figure 1. Top: Cross section of tissue surrounded by a box of blood. Bottom: corresponding top view including exemplary bipolar electrode pairs (red: injecting; black: measuring) using horizontal, vertical, and spline patterns on, from left to right: homogeneous healthy tissue, homogeneous scar tissue, and healthy tissue with a line of scar.

noted as d_T, the catheter-tissue distance ranged from 0 to 2 mm in steps of 0.5 mm. For the multielectrode grid setup, a 4×4 configuration with spacing between electrodes $d_E = 4$ mm was defined. Similarly, the star-shaped catheter was implemented using five concentric circles of radii $r_C = \{2.5,5,7.5,10\}$ mm with the electrodes placed at $\alpha_E = \{0,72,144,216,288\}°$.

Three different tissue configurations depicted in Figure 1 were employed, encompassing homogeneous physiological tissue, homogeneous scar tissue, and a central transmural scar line with a width of 8 mm flanked by healthy myocardium.

Mesh resolution of blood and tissue elements was adapted to be the highest surrounding the electrodes (ca. 0.15 mm edge length) and close to the tissue surface, while it decreased for larger distances to the catheter, with an average of 1.53 mm.

2.2. Forward Simulation

The local electric impedance simulation was performed as described previously [5]. In brief, the electric field was simulated using the software EIDORS [7] in MATLAB (MathWorks, version 2023b). An alternating current of 5 μA peak-to-peak amplitude at 14.5 kHz was simulated. Conductivity values at body temperature and f = 14.5 kHz were assigned to each tetrahedral element of the mesh: 0.7 S/m for blood, 0.164 S/m for healthy tissue, and 0.387 S/m for scar tissue.

For the squared catheter, a total of eight different bipolar pairs were employed. A four electrode circuit was always used, meaning that two electrodes formed the injecting bipole and the potential difference was measured between another two electrodes. The horizontal patterns in which the electrodes were aligned in the same row used the outer electrodes as the stimulating pair and the inner electrodes as the measuring pair. Similarly, for the vertical patterns, the employed electrodes were aligned in the same column, where the stimulating electrodes were placed at the top and bottom and the measurement electrodes in the internal part. For the star catheter, five different bipolar pairs using a single spline each time were simulated. At each spline, the electrodes located at the ends were used as the stimulating pair and the potential difference was measured between the encompassed two electrodes on the same spline. An exemplary bipolar pair of each configuration, namely horizontal, vertical, and spline, is depicted in the bottom part of Figure 1.

Combining 13 stimulation patterns, five catheter-tissue distances, and three geometrical setups, the analysis comprised 195 simulated LI measurements.

3. Results

In silico LI results for each tissue patch configuration and stimulating-measuring bipole pattern are shown in Table 1.

3.1. Catheter-Tissue Distance

Each row in Table 1 describes the results obtained for a given catheter-tissue distance. Increasing d_T yielded monotonously decreasing LI values using both catheters. The grid catheter started at a median LI value of 63.91 Ω across the eight measurements in healthy tissue at direct contact. The median LI decreased to 62.80 Ω, 60.80 Ω, 58.46 Ω, and 56.02 Ω each time the catheter moved 0.5 mm away from the tissue, respectively. This represents a 2% decrease after the first loss of contact at 0.5 mm distance, scaling to 3%, 4%, and 4% additional decrease of the LI with increasing catheter-tissue distance. Similarly, the star catheter showed a median LI value of 156.18 Ω at direct catheter-tissue contact, decreasing to 139.21 Ω, 126.64 Ω, 119.49 Ω, and 115.13 Ω at 0.5, 1, 1.5, and 2 mm distance, respectively. This decrease meant a 10%, 9%, 6%, and 4% LI drop with respect to the previous value with 0.5 mm increasing distance steps.

The decreasing LI effect can also be seen above scar tissue. At direct catheter-tissue contact, the median LI value using the grid catheter was 52.77 Ω, decreasing between 0.5 and 2% at each step, meaning 52.50 Ω, 51.76 Ω, 50.76 Ω, and 49.80 Ω, respectively. Not only the median value at direct contact, but also the drop percentage as the catheter moved away from the tissue were lower in scar tissue than in the healthy patch. When employing the star catheter, the median LI measurement at direct catheter-tissue contact with scar tissue was 130.72 Ω, decreasing to 122.44 Ω, 116.48 Ω, 113.24 Ω, and 111.28 Ω when increasing distances with 0.5 mm steps. This decrease meant a 6%, 5%, 3%, and 2% LI loss with respect to the previous value with 0.5 mm distance increasing steps.

Table 1. LI values measured *in silico* at each bipole (columns) with increasing catheter-tissue distance d_T in mm (rows) in different tissue patches: homogeneous healthy (top), homogeneous scar (middle), and healthy with a scar line (bottom).

d_T													
	LI in homogeneous healthy tissue (Ω)												
0.0	63.97	63.85	63.89	63.94	63.96	63.85	63.84	63.95	156.14	156.18	156.25	156.30	155.76
0.5	62.80	62.78	62.79	62.82	62.93	62.70	62.70	62.86	138.99	139.40	139.35	139.18	139.21
1.0	60.87	60.71	60.75	60.81	60.87	60.80	60.75	60.84	126.98	126.64	126.62	126.90	126.51
1.5	58.45	58.33	58.28	58.38	58.44	58.27	58.32	58.38	119.42	119.50	119.15	119.11	119.40
2.0	56.06	55.98	55.98	56.11	56.05	55.96	55.93	56.11	115.09	115.28	115.26	115.00	115.13
	LI in homogeneous scar tissue (Ω)												
0.0	52.81	52.73	52.77	52.79	52.81	52.73	52.72	52.81	130.72	130.72	130.75	130.80	130.38
0.5	52.57	52.48	52.49	52.50	52.59	52.45	52.41	52.53	122.25	122.60	122.56	122.44	122.43
1.0	51.81	51.69	51.72	51.76	51.81	51.76	51.72	51.78	116.81	116.48	116.44	116.71	116.35
1.5	50.84	50.74	50.69	50.77	50.83	50.68	50.73	50.77	113.25	113.34	113.00	112.94	113.24
2.0	49.83	49.76	49.76	49.87	49.82	49.74	49.72	49.87	111.25	111.43	111.41	111.15	111.28
	LI in healthy tissue with scar line (Ω)												
0.0	57.65	57.55	57.59	57.63	63.07	55.80	55.77	63.05	132.59	145.66	145.67	132.66	148.46
0.5	57.84	57.75	57.77	57.80	62.06	55.36	55.33	61.99	123.78	132.26	132.12	123.97	133.75
1.0	56.93	56.81	56.85	56.88	60.05	54.42	54.36	60.00	117.95	122.20	122.19	117.89	123.01
1.5	55.43	55.30	55.24	55.34	57.67	53.00	53.00	57.58	114.11	116.79	116.44	113.82	117.19
2.0	53.78	53.71	53.71	53.82	55.35	51.75	51.71	55.41	111.93	113.62	113.59	111.83	113.74
	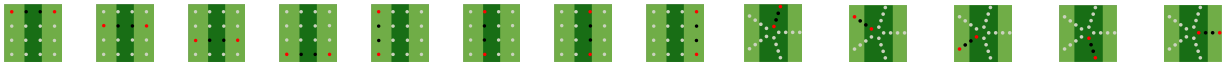												

3.2. Tissue Characterization

Theoretically, LI drops in the surrounding of myocardial scarred tissue due to the higher conductivity (lower impedance) of scar tissue in comparison to healthy myocardium. In this work, scar tissue always yielded lower LI values than healthy scenarios for both catheters and all stimulating bipoles used. When comparing median measurements at direct catheter-tissue contact, LI in healthy tissue exceeded the value in scar tissue by 17% and 16% using the grid and the star catheters, respectively.

Using the grid catheter and when a transmural scar line of 8 mm width was present, overall, the median LI value across all adjacent bipoles at direct catheter-tissue contact was 58.5 Ω, which was 9% lower than for myocardial tissue and 10% higher than for scar tissue. This median value therefore lies in between the measured values on homogeneous tissue patches. Similarly with the star catheter, the median LI value at direct catheter-tissue contact was 145.66 Ω, which was 7% lower than for myocardial tissue and 10% higher than for scar tissue, laying in between the obtained measurements on tissue patches with homogeneous conductivity.

Accounting for the location of bipolar pairs, horizontal bipoles on the grid catheter recorded their respective LI measurements across the scar line, whereas vertical pairs were located completely on either healthy or scar tissue. Horizontal pairs measured on average 57.61±0.04 Ω at direct contact. These measurements were in line with LI values being in between healthy and scarred tissue. On the contrary, vertical pairs showed clear differences between the outer adjacent pairs measuring 63.1 Ω and the internal adjacent pairs, obtaining 55.8 Ω which matches the expected values according to the tissue beneath the electrodes involved. However, the star catheter has a smaller interelectrode distance and spanned across the scar tissue line with at least two electrodes located fully on scar.

4. Discussion

In this work, previous studies using ablation catheters were extended to multielectrode mapping catheters. Increasing the catheter-tissue distance and changing the conductivity of the patch from healthy myocardium to scar tissue, yielded differences in the *in silico* LI values observed.

It is important to take into account the differences in interelectrode distance, which yields to a different field of view among catheters and thus, distinct order of LI measurements. Simulated LI in [5] yielded LI values exceeding bloodpool by 16% and 14.9% at direct catheter-tissue contact using ablation catheters with a d_E distance between 6 and 7 mm, respectively. In this work, LI measured with a grid catheter with d_E =4 mm showed a bloodpool value of 45.53 Ω, increasing by 28.82% at direct catheter-tissue contact. Similarly, starting from a bloodpool value of 108.06 Ω using a star catheter with d_E =2 mm, LI increased 31% when reaching direct catheter-tissue contact. In this work, LI measured at the furthest tested distance on healthy tissue never reached the LI measured at direct

contact in homogeneous scar tissue, being approximately 3 Ω (5%) higher compared to direct contact in homogeneous healthy tissue. Using a grid catheter, the simulated LI values never overlapped between measurements on homogeneous healthy and scar tissues. However, that was not the case for the star catheter, where LI simulated at direct catheter-tissue contact on homogeneous scar tissue were in between the values obtained at increasing catheter-tissue distance on healthy myocardium. In particular, LI measured at 0 mm distance on scar tissue yielded similar results than on healthy tissue in between 0.5 and 1 mm distance, being 8 Ω lower and 4 Ω higher, respectively.

In [5], the direct catheter-tissue contact at the center of a scar tissue line of 6 mm width yielded to 6% and 5.7% decrease with respect to the value measured at healthy tissue. In this work, the decrease in LI measured in scar tissue with respect to healthy myocardium yielded an average decrease of 17% and 16% for the grid and the star catheter, respectively.

Due to differences in d_T between the grid and the star catheter, the presence of a scar line altered the LI measurements compared to the healthy homogeneous tissue patch in a different order of magnitude. Depending on the location and direction of the measuring and stimulating patterns, the results for the grid catheter were closer to those obtained on healthy myocardium than on scar tissue. As it can be seen in the first four columns of Table 1, injected current through horizontal bipoles crossed the scar line, yielding to LI values corresponding to the range in between healthy and scar tissue. However, vertical bipoles were located completely either on healthy or scar tissue. Outer vertical bipoles, as columns five and eight of Table 1, were located fully in healthy tissue, showing similar LI values as in a homogeneous healthy patch. On the contrary, LI measured at inner vertical pairs located on scar tissue, as described in columns five and six of Table 1, decreased in comparison to measurements taken by outer vertical pairs and horizontal pairs, showing values still far from measurements recorded on homogeneous scar tissue. Due to the reduced interelectrode distance of the star catheter in comparison to the grid, the line of scar covered a larger portion of the catheter and thus yielded similar results as in the homogeneous scar setting. Within the star catheter, the innermost electrode of each spline was always located in the scar area and no pattern was purely located on healthy tissue.

The results from this work may indicate that not only the properties of the tissue directly underneath the electrodes but also a nearby area, which highly depends on the interlectrode distance of those electrodes belonging to the electrical circuit, are relevant when characterizing atrial substrate by means of LI. In this work, the grid catheter showed a field of view higher than 2 mm, whereas the star catheter interelectrode spacing had a field of view close to 2 mm. The electrode size and orientation, together with the catheter geometry, can be crucial for identifying potentially arrhythmogenic areas.

5. Conclusions

The resulting environment and simulations represent a valuable starting point to further study the incorporation of LI into the clinical mapping field and assist future catheter development by understanding the effects of scar tissue, catheter-tissue distance, and electrode arrangement.

Acknowledgments

This work was supported by the European Union's Horizon 2020 research and innovation programme under the Marie Skłodowska-Curie grant agreement No 860974 (PersonalizeAF). Authors thankfully acknowledge the valuable feedback of Marie Houillon on this manuscript.

References

[1] Nairn D, Eichenlaub M, Müller-Edenborn B, et al. Differences in atrial substrate localization using late gadolinium enhancement-magnetic resonance imaging, electrogram voltage, and conduction velocity: a cohort study using a consistent anatomical reference frame in patients with persistent atrial fibrillation. Europace 8 2023;25(9).

[2] Sulkin MS, Laughner JI, Hilbert S, et al. Novel measure of local impedance predicts catheter–tissue contact and lesion formation. Circ Arrhythmia Elec 2018;11(4):e005831.

[3] Martin CA, Martin R, Gajendragadkar PR, et al. First clinical use of novel ablation catheter incorporating local impedance data. J Cardiovasc Electr 9 2018;29(9):1197–1206.

[4] Martínez Antón C, Sánchez J, Heinkele A, et al. Effect of contact force on local electrical impedance in atrial tissue - an in silico evaluation. In 2022 Comput Cardiol (CinC), volume 498. 2022; 1–4.

[5] Unger LA, Martínez Antón C, Stritt M, et al. In silico study of local electrical impedance measurements in the atria - towards understanding and quantifying dependencies in human. IEEE Trans on Biomed Eng 2023;70(2):533–543.

[6] Unger LA, Schicketanz L, Oesterlein T, et al. Local electrical impedance mapping of the atria: Conclusions on substrate properties and confounding factors. Frontiers Physiol 2022; 12:788885.

[7] Adler A, Lionheart WRB. Uses and abuses of EIDORS: an extensible software base for EIT. Physiol Meas 5 2006; 27(5):S25–42.

Address for correspondence:

Carmen Martínez Antón, publications@ibt.kit.edu
Institute of Biomedical Engineering, Karlsruhe Institute of Technology (KIT), Kaiserstr. 12, 76131, Karlsruhe, Germany